universidad SANJORGE GRUPO SANVALERO

1. Cardiac Modeling

Biomathematics

Jesús Carro
jcarro@usj.es
22nd June, 2022

Contents

Content

1 Motivation

According to data from the World Health Organization (WHO), 17.7 million people were estimated to have died of cardiovascular diseases (CVDs) in 2015. This represents 31% of all global deaths, making CVDs the leading cause of death worldwide. CVDs are caused by different disorders of the heart and blood vessels, which include coronary heart disease (heart attacks), cerebrovascular disease (stroke), raised blood pressure (hypertension) or peripheral artery disease. Of note, CVDs are the leading noncommunicable diseases (NCDs). In 2011, 36 million people died from NCDs, with half of them caused by CVDs [1]. Improvement of the current techniques to detect, diagnose and prevent CVDs is, thus, necessary.

Among CVDs, an important percentage of deaths are related to cardiac arrhythmias, some of which may lead to sudden cardiac death. Arrhythmias are defined as irregularities in the heartbeating. The abnormal rhythm of the heart may be associated with the heart beating too quickly, too slowly or erratically. Different types of cardiac arrhythmias include atrial fibrillation, conduction disorders, premature contractions, ventricular tachycardia or ventricular fibrillation, to name a few. Cardiac arrhythmias can be caused by an abnormal behavior of the heart's natural pacemaker, a problem in the conduction system of the heart or because another part of the heart starts working as the pacemaker, among others. In those situations the heart may be precluded from carrying out its main function: to pump deoxygenated blood to the lungs and oxygenated blood to the rest of the body.

The heart is a complex system that works through the interaction of a large number of elements acting at different scales. The main function of the heart is mechanical, with this action being electrically controlled. Mathematical modeling and simulation of the heart's electrical activity (so-called cardiac electrophysiology) combined with signal processing of bioelectrical signals provide an ideal framework to join the information from clinical and experimental studies with the understanding of the mechanisms underlying them.

In a relatively near future, those tools might be used in the clinical practice as complementary instruments to help in the prevention of cardiac diseases and in the improvement of their diagnosis and therapy. In particular, cardiac *in silico* modeling and simulation could improve our understanding of the heart's function, the generation of different pathologies and their associated manifestations. To that end, it is essential to have action potential (AP) models able to reproduce experimentally and clinically observed behaviors at the cell and tissue levels. This would allow simulation of the electrical activity of the heart from the cell to the body surface and *in silico* reconstruct the most commonly used bioelectrical signal in the clinics, the electrocardiogram (ECG). The developed models could subsequently be used to investigate, for instance, the mechanisms and manifestations of ventricular arrhythmias at different scales, which is a major focus of the present document.

This technique needs higher mathematical capabilities, and, in this document, the key elements to understand how the mathematical modeling of the cardiac cells works will be presented. Before this, and to let the student understand the behavior of the heart, the first sections explain how the heart works (mainly from an electrical point of view), how the behavior of the heart is affected by different conditions or diseases, and, finally, how mathematical models can be used to study the heart under physiological and pathological conditions.

A description is provided on the range of involved spatio-temporal scales and on cardiac electrical propagation. Next, the evolution of cardiac electrophysiological models, the main components of a human ventricular cell model, and how they can be used to study a pathology are analyzed. Finally, some exercises are proposed based on the simulator OpenCOR to let the students analyze a simple model in an interactive way.

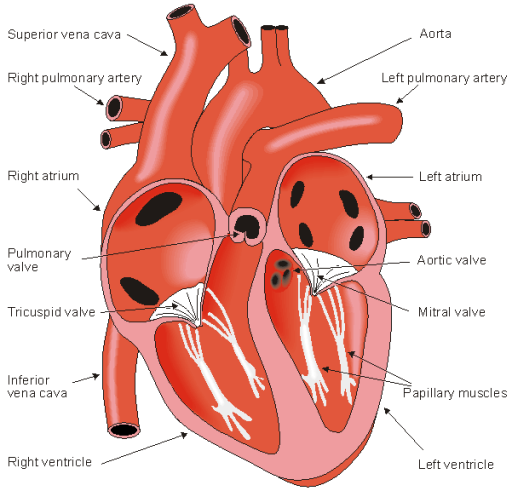

Figure 2.1: The anatomy of the heart and associated vessels. Figure from [2].

2 Electrical and Mechanical Activity of the Heart

The heart is a pump that beats around 70 times and moves more than five liters of blood per minute. It consists of four chambers: the left and right ventricles; and the left and right atria (see Figure 2.1). Deoxygenated blood enters the heart through the right atrium, and, from there, flows through the tricuspid valve to the right ventricle and is pumped to the lungs. Oxygenated blood returns from the lungs through the left atrium and then flows to the left ventricle through the mitral valve. The blood in the left ventricle is pumped through the aortic valve to the systemic circulation. Under normal conditions, all of these phases are timed and synchronized, which allows the blood to circulate and to transport oxygen and other nutrients throughout the body. This mechanism works due to the electromechanical coupling of the cardiac cells and to a complex system that propagates the electrical signals in such a way that facilitates a coordinated contraction of the heart.

2.1 EXCITABILITY OF CARDIAC CELLS

Atrial and ventricular muscle cells (or cardiomyocytes) are excitable cells. As such, when a stimulus current pulse depolarizes the resting membrane of a cardiomyocyte beyond the threshold voltage, an AP is generated. During an AP, the membrane potential (the potential at the inner surface relative to that at the outer surface of the membrane) rises rapidly at the beginning (depolarization). This first depolarization phase is followed by a small decrease in the AP (dome) to subsequently enter the third phase (plateau) where the membrane potential is held at a high voltage for some milliseconds. During the fourth phase (repolarization), the membrane potential recovers its resting value, corresponding to the fifth and last phase.

The AP is generated by concentration differences between the ions in the intracellular and extracellular compartments. In the case of atrial and ventricular myocytes, the three main ions are sodium (Na^+), potassium (K^+) and calcium (Ca^{2+}). When an external stimulus is applied to an atrial or ventricular myocyte, an initial upstroke is generated by the inward flux of sodium ions through the sodium channels. After the first phase, sodium channels close and the transient outward potassium current is activated and attempts to return the cell to its resting state. This action is counteracted by an inward calcium ion flux, which in combination with the action of potassium currents contribute to keep the potential approximately constant during the *plateau* phase. Calcium channels start to close while slow potassium currents remain active until the cell recovers its initial resting state. In cardiac muscles, excitation of one cell can propagate to the neighboring cells, and, as a result, the concurrent activation generates complex wavefronts that propagate through the cardiac tissue.

2.2 ELECTROMECHANICAL COUPLING

Upon depolarization of an atrial or ventricular cardiomyocyte's membrane, the channels allowing the passage of calcium ions become open. Most of these ions enter through L-type calcium channels to a subspace called the dyadic space, which is formed by the T-tubule (an extension of the cell membrane) and the close proximity of the sarcoplasmic reticulum (the internal store for calcium). When calcium enters, the concentration in the dyadic space rises and it triggers the opening of the ryanodine receptors in the sarcoplasmic reticulum. This launches a process known as calcium-induced calcium-release, during which the calcium input into the cell is amplified with the calcium released from the sarcoplasmic reticulum (SR). Part of the calcium in the cytosol is buffered to troponin and calmodulin. Binding of calcium to troponin favors myofilament contraction. The joint action of many cardiac cells contracting in an orderly way in a small period of time allows blood to be pumped by the heart.

2.3 PROPAGATION OF THE ELECTRICAL SIGNAL THROUGHOUT THE HEART

As described in previous sections, cardiac tissue is electrically excitable and excitation propagates throughout the heart. Excitation of cardiac tissue triggers contraction in association with the electromechanical coupling referred above. Both electrical and mechanical phenomena are fundamental for heart's functioning, together with proper synchronization of the activity corresponding to different cardiac regions.

The *pacemaker* of the heart is the sinoatrial (SA) node, which is located in the right atrium, specifically lying at the junction of the right atrium and the superior vena cava. It consists of specialized self-excitatory muscle cells that are self-activated at a rate of about 70 beats per minute. From the SA node, activation propagates throughout the atria. Before proceeding to the ventricles, activation propagates through the atrioventricular (AV) node, located at the boundary between the atria and the ventricles. Since conduction velocity (CV) in the AV node is very low (2-5 cm/s, while CV in the atria is between 50 and 100 cm/s) [2], excitation of the ventricular tissue is delayed. Specifically, the activation wavefront is estimated to take approximately 75 ms to cross the AV node. Because of this, the atria contract and pump the blood to the ventricles when these are still relaxed.

Once the activation traverses the AV node, it travels through a *common bundle*, called the *bundle of His*, which is later divided into two bundle branches: the *right* and *left bundle branches*. Finally, these branches ramify into the *Purkinje fibers*, which are connected to the ventricles and allow activation to be spread throughout the ventricles from many different locations. Following electrical activation, the ventricles contract and pump out the blood to the lungs and the rest of the body.

Figure 2.2 illustrates isochronic surfaces of ventricular electrical activation. The image is from [2], with data from [3].

Electrical signals, APs, corresponding to various regions in the heart are shown in Figure 2.3. As can be observed from the figure, these present different shapes. Figure 2.3 illustrates these APs with delays similar to those reported for a healthy heart.

2.4 THE ELECTROCARDIOGRAM

The ECG is a tool commonly used to assess the electrical and muscular activities of the heart. It records the electric potential on the surface of the thorax generated by the electrical activity of cardiac cells. To acquire an ECG, electrodes are placed on the thorax to record various electric signals at different positions. In figure 2.4 the standard 12-lead ECG is presented.

As depicted in Figure 2.3, depolarization and repolarization of cardiac cells is represented in the following waveforms of the ECG:

- Atrial depolarization corresponds to the P-wave.

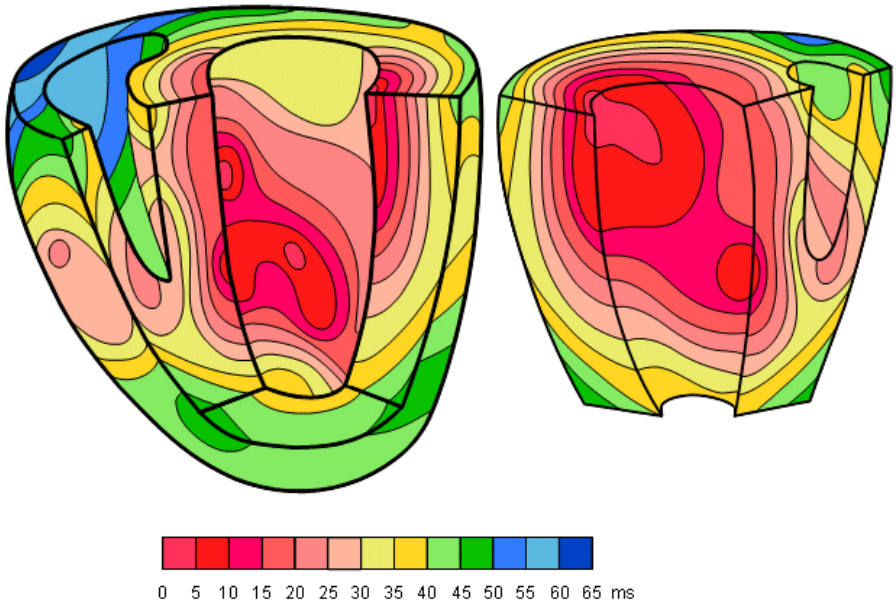

Figure 2.2: Isochronic surfaces of ventricular activation. Image from [2], with data from [3].

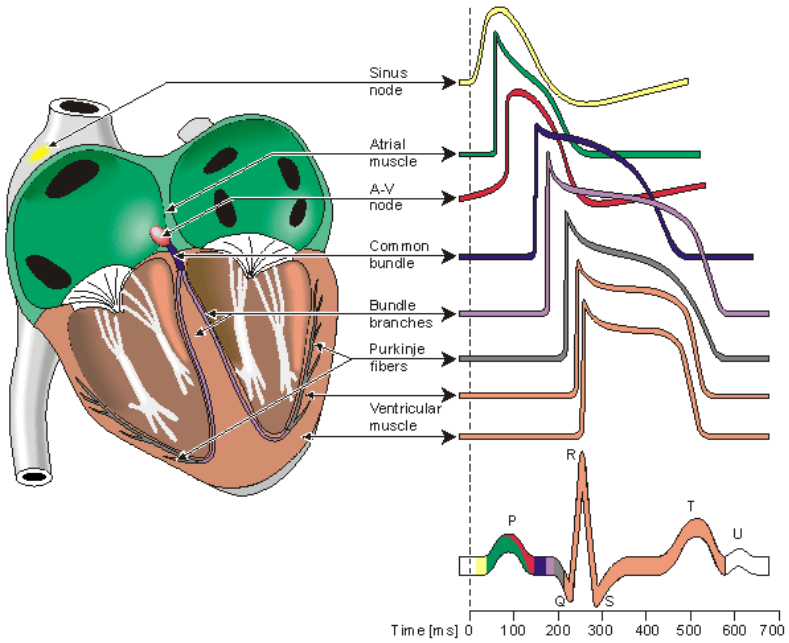

Figure 2.3: AP waveforms for cells in different regions of the heart presented with delays similar to those reported for a healthy heart. Image from [2].

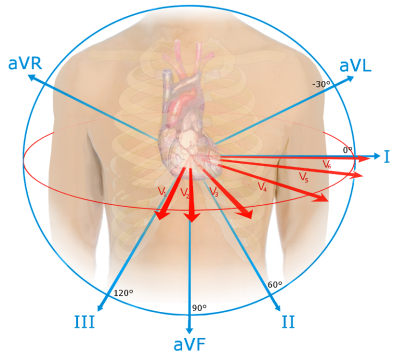

Figure 2.4: Electrode positions in the standard 12-lead ECG. Image created by Nicholas Patche, Boston Medical Center (CC BY-SA 4.0).

- Ventricular depolarization corresponds to the QRS-complex, which also contains atrial repolarization.
- Ventricular repolarization corresponds to the T-wave.

The use of the ECG is widespread in clinical practice, as it is a non-invasive test that provides significant information about cardiac electrical events. It should be noted that the ECG offers simultaneous information at different spatio-temporal scales. In many instances, some information of interest could thus be masked by other events in the heart or by the effect of propagation. ECG processing combined with in-silico modeling and simulation of cardiac electrical activity represent a powerful tool to improve our current understanding of heart's functioning and its manifestations at the surface of the thorax, as it is possible to simultaneously analyze the ECG and the underlying electrical signals at different scales.

3 Modeling the electrical activity of the heart

Cardiac electrophysiological models can be used to simulate the electrical activity of a cardiomyocyte, a fiber of cells, a piece of tissue or the entire heart. This wide range of possibilities makes them very useful for research in many different situations and for many purposes. Some of the benefits of using cardiac modeling and simulation are described in the following, together with potential associated shortcomings one should be aware of:

- *Increase knowledge on cardiac electrophysiology*: In certain *in vivo* or *in vitro* experiments only a few variables of interest can be concomitantly measured during the experiment. *In silico* modeling and simulation of cardiac electrical activity allows simultaneous exploration of all variables of interest, thus leading to improved understanding of the mechanisms underlying healthy and pathological behaviors. Nevertheless, given that models may be limited in accurately representing biological behavior, either because of lack of knowledge or impossibility to account for all the complexity in model descriptions, their use should always be accompanied by awareness of their limitations and consideration of the research objective they could contribute to.
- *Assist in decision making*: Cardiac computational models of specific pathologies, accounting for well-known high inter-patient variability, can be built. These models can be used in a wide range of applications, like drug testing or assessment of ablation effects, to name a few. As a result, both beneficial and detrimental consequences of evaluated treatments could be identified, which could, in turn, guide novel experimental and clinical evaluations.

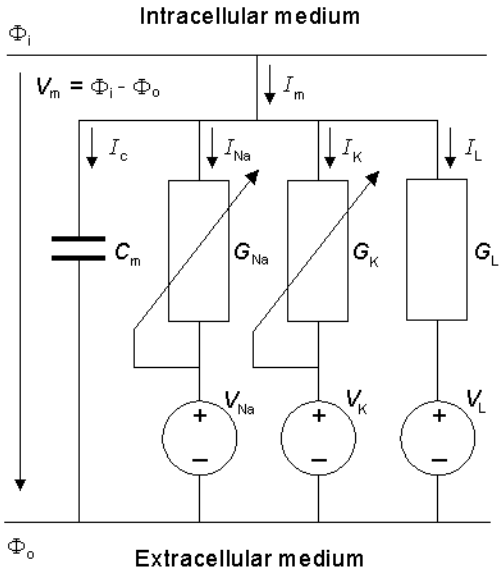

Figure 3.1: The equivalent circuit of the Hodgkin-Huxley model. The voltage sources show the polarity of the positive value. The calculated Nernst voltages of sodium, potassium and chloride designate the value of corresponding voltage sources. Image from [2].

- *Reduce animal experimentation*: Development of novel drug compounds requires different levels of testing to assess potential cardio-toxic effects. Modeling and simulation of cardiac electrical activity represents an alternative to current animal experiments.

3.1 FIRST ELECTROPHYSIOLOGICAL MODEL OF AN EXCITABLE CELL

The first computational model of the AP was proposed by Alan L. Hodgkin and Andrew F. Huxley [4]. This model was introduced to explain experimental measurements of the electrical activity of the squid giant axon obtained using the voltage clamp technique. In the proposed model, the cell was described as an electrical circuit in which ionic currents pass through ion channels that act as resistances, with the cell membrane acting as a capacitor. The electrical activity of the squid giant axon was described by four currents: a sodium current (I_{Na}), a potassium current (I_K), a small *leakage current* (I_l), which represents the current carried by other ions (mainly chloride ions), and the capacitive current. Each of these currents uses its own path or channel in the cell and, for this reason, this model is called the *parallel conductance model* or the *chord conductance model* [5]. In the original formulation of the *Hodgkin-Huxley* (HH) model, a current from the outside to the inside was represented as a positive current. In this document the most conventional notation currently in use, which represents a current from the inside to the outside as a positive current, is employed [2] (see Figure 3.1).

Two forces move the ions into or out of the cell, namely diffusion force and electrical force. For a given type of ion, when these two forces are equal in magnitude but opposite in sign, the ion is in equilibrium. The equilibrium potential of an ion is called the *Nernst potential* and is defined as follows [6]:

$$V_k = -\frac{R \cdot T}{z_k \cdot F} \log\left(\frac{[k]_i}{[k]_o}\right) \tag{3.1}$$

where V_κ is the Nernst potential for ion k, R is the gas constant, T is the absolute temperature, z_k is the valence of ion k, F is the Faraday's constant, $[k]_i$ is the intracellular concentration of ion k, and $[k]_o$ is the extracellular concentration of ion k. For the diffusion force in the HH model, a voltage source is considered and the Nernst potential is used. The ion permeability of the membrane for the different ions is taken into account by defining a conductance per unit area (based on Ohm's law) as follows:

$$G_\kappa = \frac{I_k}{V_m - V_\kappa} \tag{3.2}$$

where G_κ is the membrane conductance per unit area for ion k, I_k is the electric current carried by ion k per unit area, V_κ is the Nernst potential for ion k and V_m is the membrane voltage.

In the HH model, formulations are correspondent with the fact that each type of ion passes only through channels that are specific for it. Hodgkin and Huxley assumed that the opening and closing of the channels are controlled by electrically charged particles. The probability that one of these particles is in an open state depends on the membrane voltage. Thus, the ionic conductance for each channel was defined as the product between the maximal conductance of the channel (a constant value) and the fraction of particles in the open state. No assumption on the chemical or anatomical nature of these particles was made [2]. The fraction of particles in the open state was mathematically modeled by using ordinary differential equations as follows:

$$\frac{dg}{dt} = \alpha_g \cdot (1 - g) - \beta_g \cdot g \tag{3.3}$$

where α_g is the transfer rate coefficient for particles from closed to open state, β_g is the transfer rate coefficient for particles from open to closed state, g is the fraction of particles in the open state and $(1-g)$ is the fraction of particles in the closed state. By using the previous equation, the steady-state values of the fraction of particles in the open state and the constant time needed to reach steady-state can be obtained:

$$g_{ss} = \frac{\alpha_g}{\alpha_g + \beta_g} \tag{3.4}$$

$$\tau_g = \frac{1}{\alpha_g + \beta_g} \tag{3.5}$$

For a voltage-clamp experiment, the fraction of particles in the open state will follow the expression:

$$g(t) = g_{ss} + (g_{ss} - g_0) \cdot e^{-\frac{t}{\tau_g}} \tag{3.6}$$

where g_0 is the fraction of particles in the open state at the beginning of the experiment.

According to the definition proposed by Hodgkin and Huxley, each channel can have more than one type of particles and can need more than one particle in the open state to allow ions to pass through it. For example, in the HH model, potassium channels are formed by four particles of type n, while sodium channels are formed by three particles of type m and one of type h. The potassium and sodium conductances in the HH model are defined as follows:

$$G_\kappa = G_{K,max} \cdot n^4 \tag{3.7}$$

$$G_{Na} = G_{Na,max} \cdot m^3 \cdot h \tag{3.8}$$

where $G_{K,max}$ and $G_{Na,max}$ are the maximal conductances of the potassium and sodium channels, respectively.

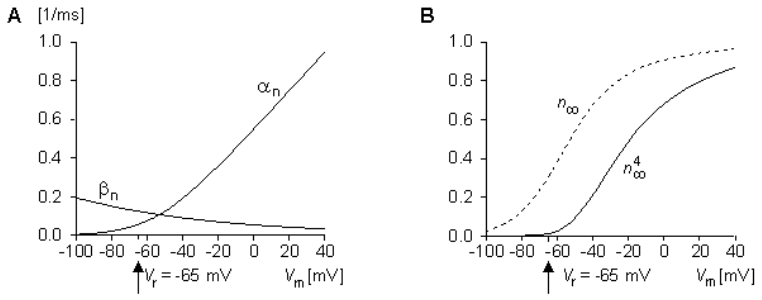

Figure 3.2: Voltage dependence of particles in the potassium channels of the HH model. (A) Variation of transfer rate coefficients α_n and β_n, (B) variation of n and n^4 as functions of membrane voltage. Image from [2].

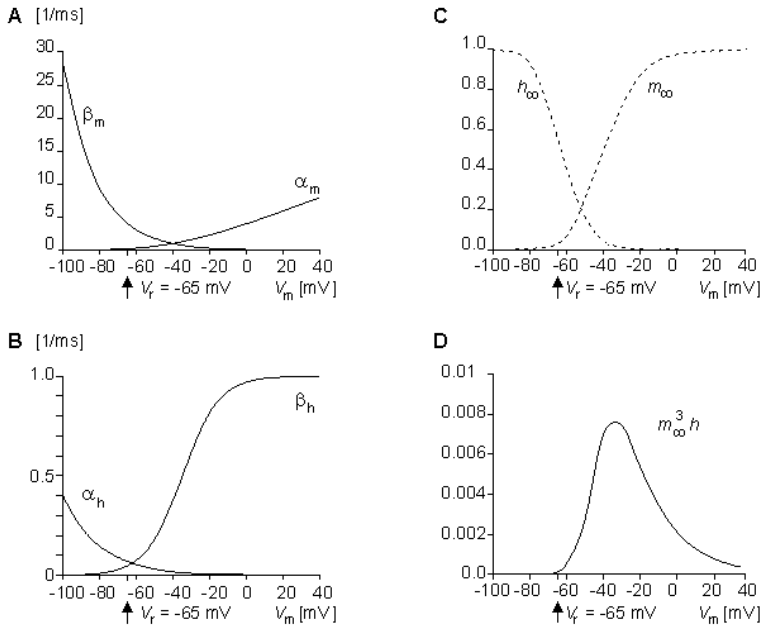

Figure 3.3: Voltage dependence of particles in the sodium channels of the HH model. (A) α_m and β_m, (B) α_h and β_h, (C) m and h and (D) $m^3 \cdot h$ as functions of membrane voltage. Image from [2].

The particles of type n and m are particles of activation. At the resting membrane potential they are not in the open state and when voltage increases, the fraction of particles in the open state increases (see Figure 3.2 and Figure 3.3). On the other hand, the particles of type h are particles of deactivation. When voltage tends to minus infinity, all the particles are in the open state but when voltage increases, the fraction of particles in the open state is reduced (see Figure 3.3).

The total transmembrane current density in the HH model is the sum of the capacitive and ionic currents as follows:

$$I_m = C_m \cdot \frac{dV_m}{dt} + (V_m - V_{Na}) \cdot G_{Na} + (V_m - V_K) \cdot G_K + (V_m - V_L) \cdot G_L \qquad (3.9)$$

where I_m is the membrane current per unit area; C_m is the membrane capacitance per unit area; V_m is membrane voltage; V_{Na}, V_K and V_L are the Nernst potential for sodium, potassium and other ions (leakage voltage), respectively; and G_{Na}, G_K and G_L are the sodium, potassium and leakage conductances per unit area, respectively.

When the cell is in an open circuit, there cannot be axial current since there is no potential gradient in the axial direction. Under this situation, the previous equation can be expressed as follows:

$$\frac{dV_m}{dt} = -\frac{1}{C_m} \cdot ((V_m - V_{Na}) \cdot G_{Na} + (V_m - V_K) \cdot G_K + (V_m - V_L) \cdot G_L) \tag{3.10}$$

3.2 EVOLUTION OF ELECTROPHYSIOLOGICAL MODELS FOR CARDIAC CELLS

The formalism introduced by Hodgkin and Huxley continues to be used today and most electrophysiological models developed after Hodgkin and Huxley, including cardiac models, follow this formalism.

Ten years after the HH model was published, Denis Noble proposed the first mathematical model of a cardiac cell in which he adapted the HH model to represent the electrophysiological behavior of a Purkinje cell [7]. The first cardiac electrophysiological models were developed to explain the main differences between cardiac and nerve cells and, specifically, the AP duration [8]. Soon, these models became more complex by incorporating the different ionic currents that were being discovered. Initially, the potassium current was separated into two new currents: I_{K1} and I_{K2} [9–11]. Later, Sanguinetti and Jurkiewicz discovered that the I_{K2} current was made up of two components: I_{Kr} and I_{Ks} [12]. However, it was not until 1964 that voltage-clamp experiments allowed the discovery of the calcium current [13]. Step by step, other elements were incorporated into the models, as the *sodium-calcium exchanger* current (I_{NCX}) and homeostasis of intracellular concentrations [14]. Similarly, mathematical models were adapted to different cell types: ventricular [15] or atrial [16]; and different species: rabbit [16, 17], guinea pig [18, 19], dog [20, 21] or human [22–25].

Cellular AP models can be incorporated into one-, two- or three-dimensional models to simulate propagation in a piece of cardiac tissue or the whole heart [26–29] and study pathologies or treatment effects.

3.3 HUMAN VENTRICULAR ELECTROPHYSIOLOGICAL MODELS: MAIN IONIC CURRENTS

A cardiac electrophysiological model describes the temporal evolution of the membrane potential of a cardiac cell and is composed of different currents that pass through the cell membrane. As described for the HH model, these currents are generated by the passage of ions through different channels, exchangers and pumps that connect the intracellular and the extracellular media. Each current is formulated mathematically to represent the various events that occur in relation to the channels (for example, activation and inactivation of ion channels). These models also include the balance between the intracellular and extracellular ionic concentrations and between the different compartments of the myocyte. In the case of human ventricular AP models, the most relevant ions are: sodium (Na^+), potassium (K^+) and calcium (Ca^{2+}). While there are many differences between the existing human ventricular cell models, the main ionic currents are present in all of them. In the following subsections, these currents are described.

Sodium current

The fast sodium current (I_{Na}) is the main sodium current in human ventricular cells. There exists also the late sodium current (I_{NaL}). Although some studies have suggested that this late sodium current plays a relevant role only under pathological conditions, like LQT3 or HF [30], this is still a matter of debate. In most human ventricular AP models, I_{Na} is modeled following the formalism proposed by Hodgkin and Huxley, with three activation gates of type *m* and two inactivation gates (*j* and *h*).

Potassium currents

Four potassium currents are mostly present in human ventricular cell models. Three of them correspond to voltage-gated ion channels (K_V), whereas the fourth one is an inward rectifying current. K_V channels are the most diverse super-family of ion channels and have a significant impact on AP shape and duration. Differences in K_V channels have been related to the cell type and function, but also to differences among various species [30]. These differences highlight the importance of using data from human cardiomyocytes for characterization of these currents.

Transient outward potassium current (I_{to}):

This voltage-gated current activates and inactivates rapidly during the depolarization phase of the action potential. It can be divided into two components ($I_{to,f}$ and $I_{to,s}$). Both components activate rapidly following membrane depolarization. On the other hand, $I_{to,f}$ inactivates rapidly, whereas $I_{to,s}$ inactivates slowly. While not all published human ventricular AP models divide the current into two components, all define it with two voltage-dependent gates (one for activation and another one for inactivation). The major difference between models lies in how they model variability between ventricular cell types: by varying the conductance, by modifying the proportion of the fast and the slow component or by a combination of both.

Rapidly activating delayed rectifier potassium current (I_{Kr}):

This current activates upon depolarization and is rapidly inactivated. Its activation is notably slower than its inactivation ($\tau_{act} > 100ms$, $\tau_{inact} < 20ms$) [30]. In recent human ventricular cell models, this current is modeled by using two voltage-dependent gates (one for activation and another one for inactivation) following the HH formalism.

Slowly activating delayed rectifier potassium current (I_{Ks}):

This slow component of the total potassium current is much smaller than I_{Kr} and plays a less significant role in modulating the AP duration (APD) [31]. When this current is blocked, and in the absence of sympathetic stimulation, the role played by I_{Ks} is relatively small. However, when ventricular repolarization reserve is attenuated, the role of this current in limiting AP prolongation becomes significant [32]. This current is generally modeled using the HH formalism with two voltage-dependent activation gates. In most models, the two voltage-dependent gates are equal.

Inward rectifier potassium current (I_{K1}):

This current is present in all ventricular and atrial myocytes and plays a major role in AP repolarization [33]. It is usually modeled using the HH formalism with one voltage-dependent and time-independent gate.

Calcium current

The *L-type calcium current* (I_{CaL}) is the principal current for the entry of calcium in cardiac cells. It is typically modeled using the *Goldman-Hodgkin-Katz* equation. This current plays an important role during the *plateau* phase of the AP and in modulating the APD and the repolarization shape. The L-type calcium channels are commonly modeled by a voltage-dependent activation gate (d), one or more voltage-dependent inactivation gates (f, $f2$) and calcium-dependent inactivation gates.

Pumps and exchangers

The above described currents correspond to currents associated with the ions passing through ion channels without requiring energy expenditure. However, there are also currents in the cell caused by the movement of ions against gradient that require ATP consumption (pumps) or by using the force of ions that pass in the direction of the gradient (exchangers). Two of these types of currents, namely the sodium-potassium pump current and the sodium-calcium exchanger current, are present in most human ventricular cell models.

Sodium-potassium pump current (I_{NaK}):

The sodium-potassium pump current is the principal mechanism for active ion transport across the membrane of excitable cells [34]. In addition, it plays an important role in regulating cardiac electrophysiology under physiological and pathological conditions. Two schemes have become predominant for modeling this current: the first one proposed by Di Francesco and Noble in their seminal work [14] and the second one described in the work by Luo and Rudy [35]. The DiFrancesco–Noble formulation is used in the majority of models of the specialized conduction system (sinoatrial node and Purkinje fiber models), whereas the Luo–Rudy formulation is common in mathematical models of atrial and ventricular cardiac myocytes.

Sodium-calcium exchanger current (I_{ncx}):

The sodium-calcium exchanger plays an important role in the regulation of intracellular calcium concentration ($[Ca^{2+}]_i$). This exchanger current regulates muscle relaxation in cardiac myocytes [36]. It is usually modeled following the formulation proposed by Mullins [37] and simplified by DiFrancesco and Noble [14]. In this formulation, the I_{ncx} current is modeled as a time-independent current, with the value of the current being dependent on the intracellular and the extracellular concentrations of Na^+ and Ca^{2+} ions and on the membrane potential.

3.4 HUMAN VENTRICULAR ELECTROPHYSIOLOGICAL MODELS: RECENT DEVELOPMENTS

In recent years a number of mathematical models of electrical and ionic homeostasis in human ventricular myocytes have been proposed. One of the most extensively used models is that proposed by *ten Tusscher-Panfilov* (TP06) [29], which is an improved version of the *ten Tusscher-Nobel-Nobel-Panfilov* (TNNP04) model [24], in which the calcium dynamics, the slow delayed rectifier potassium current (I_{Ks}) and the L-type calcium current (I_{CaL}) were reformulated. Both the TNNP04 and the TP06 models are based on experimental human data for most of the main ionic currents. One of the major advantages of the TP06 model over previous human ventricular models is that it accurately reproduces restitution of the APD. On the other hand, the TP06 model presents the major shortcomings of being insensitive to changes in certain ionic current densities [38] and of inadequately representing rate dependence of intracellular calcium levels [39].

Another relevant model of human ventricular cells was proposed by Iyer *et al.* (IMW04) [23]. This model provides a detailed description of calcium homeostasis and reproduces diverse aspects of the excitation-contraction coupling (ECC). However, important limitations have been reported for this model, including the fact that it is extremely sensitive to variations in I_{NaK} and I_{K1} current densities [38]. It also produces quite long APs and relatively flat restitution curves in tissue [40]. In addition, the most relevant ionic currents in the IMW04 model are described using Markovian chains, with the consequent increase in complexity (more than 60 state variables). Serious restrictions on the size of the time step required for stability and increments in the overall computational time when using this model in tissue simulations have been reported [40].

In 2010, a new model of human ventricular AP had just been proposed by Grandi *et al.* (GPB) [41]. The development of this model departs from the rabbit ECC model proposed by Shannon *et al.* [42], which includes the subsarcolemmal and junctional compartments in the formulation of the currents and provides a detailed description of calcium handling. The GPB model includes new definitions of ionic current densities and kinetics according to experimental data on human myocytes that had been recently collected. This model is defined for two types of cells, namely endocardial and epicardial. These two cell types differ only by the maximal conductivity of the fast and slow components of the transient outward potassium current (I_{to}). The GPB model improves the AP response to frequency changes and offers a better performance against blockades of potassium currents (I_{K1}, I_{Ks} and I_{Kr}) with respect to the TP06 model. The major drawback of the GPB model is that it does not adequately reproduce S1S2 restitution properties nor APD rate adaptation dynamics. These drawbacks can be attributed to the fact that the GPB model was developed from a rabbit ventricular model and the characteristics of S1S2 restitution and APD rate adaptation are notably different in the two species.

The following year, Carro *et al.* proposed a modification of the GPB model [43], the *Carro-Rodríguez-Laguna-Pueyo* (CRLP) nidek. Gating kinetics of the I_{CaL} current were reformulated by introducing both fast and slow voltage-dependent inactivation gates [29], maximal I_{NaK} was reduced to best match experimental APD_{90} rate adaptation data, and the I_{K1} current was redefined by accounting for recent experimental data published in the literature [44]. All this was developed to obtain a model suitable for the study of human ventricular electrophysiology, with a focus on the investigation of ventricular arrhythmias. This modification was based on the computation of well-established electrophysiological markers and the results of a sensitivity analysis of the modulation of those markers by variations in the characteristics of major ionic currents.

In the same year, O'Hara *et al.* proposed the *O'Hara-Virág-Varró-Rudy* dynamic (ORd) model [45]. This new ventricular cell model is based on the most extensive dataset of undiseased human cells. Data from more than 100 undiseased human hearts were used to characterize the steady-state rate dependence and restitution of the ventricular AP. The model was also evaluated under the effect of drugs that selectively block different channels, like mexiletine, ryanodine, nisoldipine and E-4031. As it will be discussed later, the complexity of this model is greater than that of previous models. The major drawback of the ORd model regards the rate dependence of the intracellular calcium ($[Ca^{2+}]_i$): While under physiological conditions $[Ca^{2+}]_i$ has been experimentally reported to increase by around 30% with frequency, in the ORd model it increases by around 300%.

In 2015, Himeno *et al.* proposed a new human ventricular membrane excitation-contraction model [46]. The Himeno et al. model included a more detailed description of the excitation-contraction coupling than previously described models and was proved to reproduce membrane excitation and calcium-induced calcium-release characteristics.

The model comparison presented in this document is restricted to the most used electrophysiological models TP06, GPB, CRLP and ORd. Table 3.1 presents a summary of the main differences between those four electrophysiological models.

	TP06	**GPB**	**CRLP**	**ORd**
# State variables	20	38	39	41
Computation time	Short	Long	Long	Long
Cell types	Endo, mid, epi	Endo, epi	Endo, Epi	Endo, mid, epi
Steady-state AP properties	Physiological APD values, very low triangulation	Physiological APD values and triangulation	Physiological APD values and triangulation	Short APD values, but physiological triangulation
Steady-state calcium levels	Low diastolic and systolic values	Very low diastolic and systolic values	Low diastolic and systolic values	Low diastolic and systolic values
APD_{90} adaptation to abrupt heart rate changes	Very fast	Rabbit characteristics	Physiological behavior	Physiological behavior
Sodium and calcium rate dependence	Very sensitive to increasing stimulation frequency	Physiological behavior	Physiological behavior	Very sensitive to increasing stimulation frequency
APD sensitivity to variations in ionic current densities	Lowly sensitive to I_{NaK}, $I_{Na,Ca}$, I_{Ks}, I_{K1}, I_{CaL}, I_{Kr} and I_{Na}	Lowly sensitive to I_{Kr} and highly sensitive to I_{K1}	Lowly sensitive to I_{Kr} and highly sensitive to I_{K1}	Lowly sensitive to I_{K1}, I_{CaL} and $I_{Na,Ca}$, and highly sensitive to I_{Kr}

Table 3.1: Differences between human ventricular cell models. Data are obtained from [38–40, 45] and from simulations performed by the author.

4 Acute myocardial ischemia

In previous sections, cardiac electrical activity under physiological conditions and the heart's primary function of pumping blood out to the body have been described. Many diseases and conditions are associated with cardiac malfunctioning. Electrical irregularities in the beating of the heart, so called arrhythmias, may lead to alterations in cardiac contraction, not allowing the heart to efficiently pump blood out to the rest of body. Some types of arrhythmias are among the most important causes of sudden cardiac death. They can be generated by abnormal automaticity, abnormal conduction of the electrical impulse or a combination of both.

Injured or damaged tissue can conduct slowly or act as an obstacle (non-conducting tissue) causing abnormal conduction. Certain channelopathies or drug effects can generate abnormal automaticity and in some cases beats may be generated in a region different from the SA node (ectopic beats). According to its origin, arrhythmias are commonly grouped into two large families: supraventricular arrhythmias and ventricular arrhythmias. Supraventricular arrhythmias occur in the upper part of the heart (above the ventricles, including the atria). On the other hand, ventricular arrhythmias occur in the lower part of the heart (the ventricles), like in the case of ventricular tachycardia or ventricular fibrillation– [47, 48]. Diverse pathological conditions can result in ventricular tachycardia or fibrillation, being acute myocardial ischemia the leading cause of ventricular fibrillation. Myocardial ischemia occurs when there is a reduction in the blood flow to the heart, usually as a result of the partial or total obstruction of one or various coronary arteries. In association with the reduction in blood flow, the flow of oxygen and glucose to cardiac muscle cells is interrupted within the affected region [49]. This situation generates three major effects: reduction in oxygen (hypoxia), increase in the extracellular potassium (hyperkalemia) and acidification of the tissue (acidosis). Under these effects, cardiac electrical activity experiences significant alterations: cell excitability and conduction velocity in tissue are reduced and the effective refractive period (ERP) is increased [49, 50]. Importantly, there is a high degree of spatial heterogeneity in these alterations, which generates a substrate for arrhythmogenesis.

Although pro-arrhythmic consequences in the setting of acute myocardial ischemia have been extensively investigated, the mechanisms underlying them are not yet fully understood. Many studies have attempted to shed light on this phenomenon by performing investigations in animal species, like pigs Janse *et al.* [51] and dogs [50]. Experimental studies have demonstrated that the above described spatial heterogeneity, particularly in the border between ischemic and healthy zones, leads to the establishment of reentries around the ischemic zone [50, 52].

At the level of the surface ECG, myocardial ischemia is clinically recognized when there is a change in the level of the ST segment [53, 54]. The mechanisms behind the ST segment change have been widely explored and there are still ongoing investigations into them. Also, other techniques have been and are being explored to increase the ability to recognize myocardial ischemia manifestations at the ECG level. Due to the complexity of the problem and the different scales involved, modeling and simulation of human ventricular electrical activity has been used to study myocardial ischemia and gain knowledge on the mechanisms underlying the initiation and maintenance of reentrant arrhythmias under myocardial ischemia.

4.1 ACUTE ISCHEMIA MODELS

Over the past 20 years, a large number of investigations have been devoted to the study of cardiac ischemia using mathematical modeling and simulation. These computational techniques have become a useful tool in analyzing electrophysiology changes associated with myocardial ischemia and the predisposition to ventricular arrhythmias [55]. In one of the first works by Ferrero *et al.* [56], the authors studied how ischemia-induced metabolic changes altered the electrophysiological behavior of cardiac tissue. This study used two-dimensional tissues, as other subsequent studies [57]. The presented research was later extended to account for heterogeneity caused by ischemia [58], realistic fiber orientation and transmural heterogeneity [59, 60]. The effect of reduced repolarization reserve in increasing arrhythmic risk in the highly heterogeneous substrate caused by acute myocardial ischemia was investigated in a recent study [61].

At the cellular level, AP is modeled under acute myocardial ischemia by adding three main effects to the ventricular electrophysiological models: hyperkalemia, hypoxia and acidosis. Hyperkalemia is simulated by increasing extracellular potassium to levels around 10 mM, in line with experimental reports [62]. Hypoxia is simulated by adding the ATP-sensitive potassium current ($I_{K_{ATP}}$), a current discovered by Noma [63]. When distribution of oxygen is reduced, the cell is not able to generate ATP from ADP. In association with this, the ATP concentration in the cell is reduced and $I_{K_{ATP}}$ channels open. Finally, acidosis is usually modeled by a reduction in the ionic conductances of I_{Na} and I_{CaL} currents according to the experimental results of [56, 64]. While all three effects are present during acute myocardial ischemia, hyperkalemia has been suggested to play the most relevant role.

For simulation of acute myocardial ischemia, a range of spatial scales may need to be considered. To investigate the increase in the effective refractory period or the decrease in the conduction velocity under ischemic conditions, one-, two- or three-dimensional tissues should be simulated. The study of reentrant patterns and vulnerable windows in acutely ischemic ventricles would benefit from analysis performed in a three-dimensional space. In this case, an ischemic region could be placed in a bi-ventricular model, which would include fiber orientation. According to the experimental findings from Coronel *et al.* [62], the ischemic region would be composed of a normal zone (NZ), transitional border zones (BZ) and the central ischemic zone (CZ). BZ could be simulated by considering a linear variation in the electrophysiological properties between NZ and CZ, in line with experiments [62]. For these simulations, an important consideration regards the washed zone in the endocardium (not affected by ischemia) as a result of the interaction between the blood inside the ventricle and the endocardial tissue [52]. In this complex scenario, the selection of the AP model is crucial. An AP model that is able to reproduce cardiac electrophysiological behavior under acute myocardial ischemia will be of utmost importance to investigate the vulnerability to ventricular arrhythmias and to elucidate the underlying mechanisms.

Practical exercises

1 OpenCOR Description

OpenCOR is a software designed for the simulation of mathematical models [65]. This simulators uses the standard CellML [66]: an open standard based on the XML markup language. CellML originated at the Auckland Bioengineering Institute at the University of Auckland, with development now led by the CellML Editorial Board.

OpenCOR is an open source project and binaries are available for Windows, Linux and Mac. You can download it from `https://opencor.ws`.

OpenCOR facilitates you to open and to modify models, using them from a perspective more focused on the equations of the model. The interface of OpenCOR permits you to see the definition of the model (Figure 1.1) and to simulate and plot the results of the model (Figure 1.2)

OpenCOR is simple to be used and, if you are familiar with the solution of ODEs, you will understand easily the different parameters you must choose. If not, we recomend you to review the course about ODEs that is also in ThinkBS.

2 Activities

To solve the following activities, you need to use the file hodgkin_huxley_1952.cellml that is with this document. In the model view you can see the different components of the model and the equations that are defined within it. You will also see the definition of the different units of the elements, and the connections between the components.

To describe completely the behavior of the program and the standard CellML is out of the scope of this document, we recommend you to review the bibliography to get more information:

OpenCOR: Garny A and Hunter P. J. *Opencor: a modular and interoperable approach to computational biology*. Frontiers in Physiology, 6, 2015. ISSN 1664-042X. doi: 10.3389/fphys.2015.00026.

CellML: Miller A. K, Marsh J, Reeve A, Garny A, Britten R, Halstead M, Cooper J, Nickerson D. P, and Nielsen P. F. *An overview of the CellML API and its imple mentation*. BMC Bioinformatics, 11(1):178, April 2010. ISSN 1471-2105. doi: 10.1186/1471-2105-11-178.

To solve it properly, select a point interval of 0.1 millisecond, the CVODE solver and a maximum step of 0.1 milliseconds in OpenCOR. If you choose to plot the variable *V* against the variable of integration (choose this option by right-clicking int the parameters windows), you should get the result of the Figure 2.1

Activity 1. Modify the HH model to simulate a periodic function

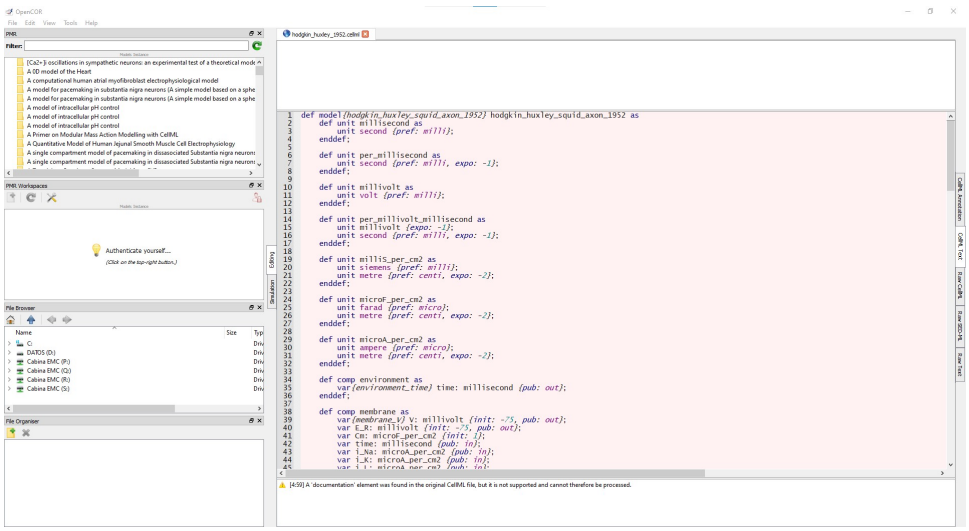

Figure 1.1: View to modify a model in OpenCOR.

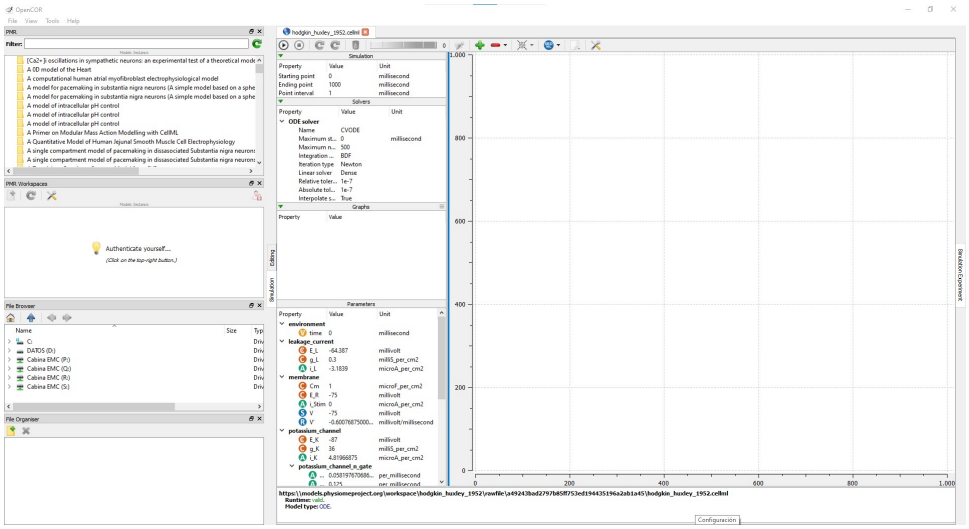

Figure 1.2: View to simulate a model in OpenCOR.

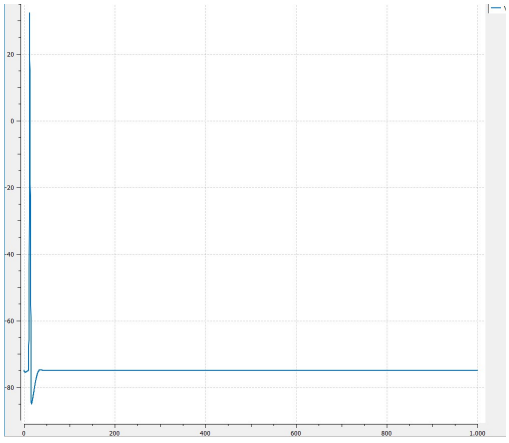

Figure 2.1: Result of the default configuration for HH model.

To do this, you can use the following code to include the Cycle Length (CL) and to modify the stimulation:

```
def comp membrane as
    var{membrane_V} V: millivolt {init: -75, pub: out};
    var E_R: millivolt {init: -75, pub: out};
    var Cm: microF_per_cm2 {init: 1};
    var time: millisecond {pub: in};
    var i_Na: microA_per_cm2 {pub: in};
    var i_K: microA_per_cm2 {pub: in};
    var i_L: microA_per_cm2 {pub: in};
    var i_Stim: microA_per_cm2;
    var CL: millisecond {init: 200};

    i_Stim = sel
        case (time - floor(time/CL)*CL >= 10{millisecond})
             and (time - floor(time/CL)*CL <= 10.5{millisecond}):
            20{microA_per_cm2};
        otherwise:
            0{microA_per_cm2};
    endsel;

    ode(V, time) = -(-i_Stim+i_Na+i_K+i_L)/Cm;
enddef;
```

What is the default CL with this code? Can you modify it to create a periodic stimulation with CL = 500 ms?

Activity 2. Modify the different maximal conductances to evaluate what happens to your results.

Activity 3. Modify the E_R potential. How does it affect to the other Nernst potentials?

Activity 4. If the extracellular potassium concentration is 5.4, can you define E_K as a function of the intracellular and the extracellular concentrations of potassium?

You need to define the two new constants, and to calculate the value of the intracellular potassium concentration to maintain the same E_K value.

Activity 5. Modify the $[K^+]_o$ value. How does it affect? Is this effect different from modifying E_R?

Activity 6. Try to find the Noble model in the Physiome repository. This model is a modification of the HH model to represent the behavior of a purkinje fiber. What are the differences in the currents that are defined? What changes does it generate?

Activity 7. Try to find any of the modern models of the human ventricle that are mentioned in this document. Can you find the different steady-state variables that are defined? How?

Bibliography

[1] Mendis S, Puska P, and Norrving B, editors. *Global Atlas on cardiovascular disease prevention and control*. World Health Organization in collaboration with the World Heart Federation and the World Stroke Organization, 2011. ISBN 9789241564373. http://apps.who.int/iris/bitstream/10665/44701/1/9789241564373_eng.pdf.

[2] Malmivuo J and Plonsey R. *Bioelectromagnetism - Principles and applications of bioelectric and biomagnetic fields*. Oxford University Press, 1995. ISBN 978-0195058239. doi: 10.1093/acprof:oso/9780195058239.001.0001.

[3] Durrer D, van Dam R. T, Freud G. E, Janse M. J, Meijler F. L, and Arzbaecher R. C. Total excitation of the isolated human heart. *Circ*, 41(6):899–912, 1970. doi: 10.1161/01.CIR.41.6.899. http://circ.ahajournals.org/content/41/6/899.

[4] Hodgkin A. L and Huxley A. F. A quantitative description of membrane current and its applications to conduction and excitation in nerve. *J Physiol*, 117(1-2): 500–544, 1952. doi: 10.1016/S0092-8240(05)80004-7. https://www.ncbi.nlm.nih.gov/pmc/articles/PMC1392413/.

[5] Junge D. *Nerve and muscle excitation*. Sinauer Associates Inc., third edition, 1992.

[6] Nernst W. Zur kinetik der lösung befindlichen körper: Theorie der diffusion. *Z Phys Chem*, 3:613–637, 1888.

[7] Noble D. A modification of the Hodgkin-Huxley equations applicable to Purkinje fibre action and pace-maker potentials. *J Physiol*, 160(21):317–352, 1962. doi: 10.1113/jphysiol.1962.sp006849. http://doi.org/10.1113/jphysiol.1962.sp006849.

[8] Noble D. Successes and failures in modeling heart cell electrophysiology. *Heart Rhythm*, 8(11):1798–1803, 2011. doi: 10.1016/j.hrthm.2011.06.014. http://doi.org/10.1016/j.hrthm.2011.06.014.

[9] Carmeliet E. E. Chloride ions and the membrane potential of Purkinje fibres. *J Physiol*, 156(2):375–388, 1961. http://www.ncbi.nlm.nih.gov/pmc/articles/PMC1359892/.

[10] Hall A. E, Hutter O. F, and Noble D. Current—voltage relations of Purkinje fibres in sodium-deficient solutions. *J Physiol*, 166(1):225–240, 1963. http://www.ncbi.nlm.nih.gov/pmc/articles/PMC1359373/.

[11] Hutter O. F and Noble D. Rectifying properties of heart muscle. *Nature*, 188 (4749):495, nov 1960. doi: 10.1038/188495a0. http://dx.doi.org/10.1038/188495a0.

[12] Sanguinetti M. C and Jurkiewicz N. K. Two components of cardiac delayed rectifier K^+ current. Differential sensitivity to block by class III antiarrhythmic agents. *J Gen Physiol*, 96(1):195–215, 1990. doi: 10.1085/jgp.96.1.195. http://jgp.rupress.org/content/96/1/195.

[13] Reuter H. The dependence of slow inward current in Purkinje fibres on the extracellular calcium-concentration. *J Physiol*, 192(2):479–92, 1967. doi: 10.1113/jphysiol.1967.sp008310. http://doi.org/10.1113/jphysiol.1967.sp008310.

[14] DiFrancesco D and Noble D. A model of cardiac electrical activity incorporating ionic pumps and concentration changes. *Phil Trans B*, 307(1133):353–398, 1985. doi: 10.1098/rstb.1985.0001. http://doi.org/10.1098/rstb.1985.0001.

[15] Beeler G. W and Reuter H. Reconstruction of the action potential of ventricular myocardial fibers. *J Physiol*, 268:177–210, 1977. doi: 10.1113/jphysiol.1977.sp011853. http://doi.org/10.1113/jphysiol.1977.sp011853.

[16] Hilgemann D and Noble D. Excitation-contraction coupling and extracellular calcium transients in rabbit atrium: reconstruction of basic cellular mechanisms. *Proc R Soc Lond B Biol Sci*, 230:163–205, 1987. doi: 10.1098/rspb.1987.0015. http://rspb.royalsocietypublishing.org/content/230/1259/163.long.

[17] Lindblad D. S, Murphey C. R, Clark J. W, and Giles W. R. A model of the action potential and underlying membrane currents in a rabbit atrial cell. *Am Physiol Soc*, 271(4):H1666–H1696, 1996. http://ajpheart.physiology.org/content/271/4/H1666.

[18] Luo C and Rudy Y. A model of the ventricular cardiac action potential: Depolarization, repolarization and their interaction. *Circ Res*, 68:1501–1526, 1991. doi: 10.1161/01.RES.68.6.1501. http://doi.org/10.1161/01.RES.68.6.1501.

[19] Noble D, Noble S. J, Bett G. C. L, Earm Y. E, Ho W. K, and So I. K. The role of sodium - calcium exchange during the cardiac action potential. *Ann New York Acad Sci*, 639(1):334–353, 1991. doi: 10.1111/j.1749-6632.1991.tb17323.x. http://dx.doi.org/10.1111/j.1749-6632.1991.tb17323.x.

[20] Winslow R. L, Kimball A. L, Varghese A, and Noble D. Simulating cardiac sinus and atrial network dynamics on the connection machine. *Physica D*, 64(1–3):281–298, 1993. doi: 10.1016/0167-2789(93)90260-8. http://doi.org/10.1016/0167-2789(93)90260-8.

[21] Ramirez R. J, Nattel S, and Courtemanche M. Mathematical analysis of canine atrial action potentials: rate, regional factors, and electrical remodeling. *Am J Physiol-Heart C*, 279(4):H1767–H1785, 2000. http://ajpheart.physiology.org/content/279/4/H1767.long.

[22] Priebe L and Beuckelmann D. J. Simulation study of cellular electric properties in heart failure. *Circ Res*, 82(11):1206–1223, 1998. doi: 10.1161/01.RES.82.11.1206. http://doi.org/10.1161/01.RES.82.11.1206.

[23] Iyer V, Mazhari R, and Winslow R. L. A. Computational model of the human left ventricular epicardial myocyte. *Biophys J*, 87(3):1507–1525, 2004. doi: 10.1529/biophysj.104.043299. http://doi.org/10.1529/biophysj.104.043299.

[24] ten Tusscher K, Noble D, Noble P. J, and Panfilov A. A model for human ventricular tissue. *Am J Physiol Heart Circ Physiol*, 286(4):H1573–1589, 2004. doi: 10.1152/ajpheart.00794.2003. http://ajpheart.physiology.org/content/286/4/H1573.

[25] Courtemanche M, Ramirez R. J, and Nattel S. Ionic mechanisms underlying human atrial action potential properties: Insights from a mathematical model. *Am J of Physiol*, 275(1):H301–H321, 1998. http://ajpheart.physiology.org/content/275/1/H301.

[26] van Capelle F. J and Durrer D. Computer simulation of arrhythmias in a network of coupled excitable elements. *Circ Res*, 47(3):454–466, 1980. doi: 10.1161/01.RES.47.3.454. http://circres.ahajournals.org/cgi/doi/10.1161/01.RES.47.3.454.

[27] Leon L. J and Horácek B. M. Computer model of excitation and recovery in the anisotropic myocardium. I. Rectangular and cubic arrays of excitable elements. *J Electrocardiol*, 24(1):1–15, 1991. doi: 10.1016/0022-0736(91)90077-Y.

[28] Trayanova N. Discrete versus syncytial tissue behavior in a model of cardiac stimulation: I. Mathematical formulation. *IEEE T Bio-Med Eng*, 43(12):1129–1140, 1996. http://ieeexplore.ieee.org/xpls/abs_all.jsp?arnumber=544337.

[29] ten Tusscher K and Panfilov A. Alternans and spiral breakup in a human ventricular tissue model. *Am J Physiol Heart Circ Physiol*, 291:H1088–H1100, 2006. doi: 10.1152/ajpheart.00109.2006. http://ajpheart.physiology.org/content/291/3/H1088.

[30] Bartos D. C, Grandi E, and Ripplinger C. M. Ion channels in the heart. *Compr Physiol*, 5(3):1423–1464, 2015. doi: 10.1002/cphy.c140069. http://doi.org/10.1002/cphy.c140069.

[31] Jost N, Virág L, Comtois P, Ördög B, Szuts V, Seprényi G, Bitay M, Kohajda Z, Koncz I, Nagy N, Szél T, Magyar J, Kovács M, Puskás L. G, Lengyel C, Wettwer E, Ravens U, Nánási P. P, Papp J. G, Varró A, and Nattel S. Molecular basis of repolarization reserve differences between dogs and man. *J Physiol*, 591:4189–4206, 2013. doi: 10.1113/jphysiol.2013.261198. http://doi.org/10.1113/jphysiol.2013.261198.

[32] Jost N, Virág L, Bitay M, Takács J, Lengyel C, Biliczki P, Nagy Z, Bogáts G, Lathrop D. A, Papp J. G, and Varró A. Restricting excessive cardiac action potential and qt prolongation. *Circ*, 112(10):1392–1399, 2005. doi: 10.1161/CIRCULATIONAHA.105.550111. http://circ.ahajournals.org/content/112/10/1392.

[33] Lopatin A and Nichols C. Inward rectifiers in the heart: An update on I_{K1}. *J Mol Cell Cardiol*, 33:625–638, 2001. doi: 10.1006/jmcc.2001.1344. http://dx.doi.org/10.1006/jmcc.2001.1344.

[34] Bueno-Orovio A, Sánchez C, Pueyo E, and Rodriguez B. Na/K pump regulation of cardiac repolarization: insights from a systems biology approach. *Pflüg Archiv*, 466(2):183–193, 2014. doi: 10.1007/s00424-013-1293-1. http://dx.doi.org/10.1007/s00424-013-1293-1.

[35] Luo C and Rudy Y. A dynamic model of the cardiac ventricular action potential: I. Simulations of ionic currents and concentration changes. *Circ Res*, 74:1071–1096, 1994. doi: 10.1161/res.74.6.7514509. https://www.ahajournals.org/doi/abs/10.1161/res.74.6.7514509.

[36] Philipson K. D and Nicoll D. A. Sodium-calcium exchange. *Curr Opin Cell Biol*, 4(4):678–683, 1992. doi: 10.1016/0955-0674(92)90089-U. http://www.sciencedirect.com/science/article/pii/095506749290089U.

[37] J M. L. A mechanism for Na/Ca transport. *J Gen Physiol*, 70:681–695, 1977. doi: 10.1085/jgp.70.6.681. http://doi.org/10.1085/jgp.70.6.681.

[38] Niederer S. A, Fink M, Noble D, and Smith N. P. A meta-analysis of cardiac electrophysiology computational models. *Exp Physiol*, 94:486–495, 2009. doi: 10.1113/expphysiol.2008.044610. http://doi.org/10.1113/expphysiol.2008.044610.

[39] Romero L, Pueyo E, Fink M, and Rodríguez B. Impact of ionic current variability on human ventricular cellular electrophysiology. *Am J Physiol Heart Circ Physiol*, 297:H1436–1445, 2009. doi: 10.1152/ajpheart.00263.2009. http://ajpheart.physiology.org/content/297/4/H1436.

[40] Bueno-Orovio A, Cherry E. M, and Fenton F. H. Minimal model for human ventricular action potentials in tissue. *J Theor Biol*, 253:544–560, 2008. doi: 10.1016/j.jtbi.2008.03.029. http://doi.org/10.1016/j.jtbi.2008.03.029.

[41] Grandi E, Pasqualini F. S, and Bers D. M. A novel computational model of the human ventricular action potential and Ca transient. *J Mol Cell Cardiol*, 48:112–121, 2010. doi: 10.1016/j.yjmcc.2009.09.019. http://doi.org/10.1016/j.yjmcc.2009.09.019.

[42] Shannon T. R, Wang F, Puglisi J, Weber C, and Bers D. M. A mathematical treatment of integrated Ca dynamics within the ventricular myocyte. *Biophys J*, 87(5):3351–3371, 2004. doi: 10.1529/biophysj.104.047449. http://doi.org/10.1529/biophysj.104.047449.

[43] Carro J, Rodríguez J, Laguna P, and Pueyo E. A human ventricular cell model for investigation of cardiac arrhythmias under hyperkalaemic conditions. *Philos T Roy Soc A*, 369(1954):4205–4232, 2011. doi: 10.1098/rsta.2011.0127. http://doi.org/10.1098/rsta.2011.0127.

[44] Fink M, Noble D, Virag L, Varro A, and Giles W. R. Contributions of HERG K+ current to repolarization of the human ventricular action potential. *Prog Biophys Mol Bio*, 96:357–376, 2008. doi: 10.1016/j.pbiomolbio.2007.07.011. http://doi.org/10.1016/j.pbiomolbio.2007.07.011.

[45] O'Hara T, Virág L, Varró A, and Rudy Y. Simulation of the undiseased human cardiac ventricular action potential: Model formulation and experimental validation. *PLOS Comput Bio*, 7(5), 2011. doi: 10.1371/journal.pcbi.1002061. http://doi.org/10.1371/journal.pcbi.1002061.

[46] Himeno Y, Asakura K, Cha C, Memida H, Powell T, Amano A, and Noma A. A human ventricular myocyte model with a refined representation of excitation-contraction coupling. *Biophys J*, 109:415 – 427, 7 2015. doi: doi:10.1016/j.bpj.2015.06.017. http://dx.doi.org/10.1016/j.bpj.2015.06.017.

[47] Zipes D. P and Wellens H. J. J. Sudden cardiac death. *Circ Res*, 98:2334–2351, 1998. doi: 10.1161/01.CIR.98.21.2334. http://doi.org/10.1161/01.CIR.98.21.2334.

[48] Rubart M and Zipes D. P. Mechanisms of sudden cardiac death. *J Clin Invest*, 115 (9):2305–2315, 9 2005. doi: 10.1172/JCI26381. https://www.jci.org/articles/view/26381.

[49] Carmeliet E. Cardiac ionic currents and acute ischemia: from channels to arrhythmias. *Physiol Rev*, 79(3):917–1017, 1999. http://physrev.physiology.org/content/79/3/917.

[50] Janse M. J and Kleber A. G. Electrophysiological changes and ventricular arrhythmias in the early phase of regional myocardial ischemia. *Circ Res*, 49(5): 1069–1081, 1981.

[51] Janse M. J, van Capelle F. J, Morsink H, Kleber A. G, Wilms-Schopman F, Cardinal R, D'Alnoncourt C. N, and Durrer D. Flow of "injury" current and patterns of excitation during early ventricular arrhythmias in acute regional myocardial ischemia in isolated porcine and canine hearts. Evidence for two different arrhythmogenic mechanisms. *Circ Res*, 47(2):151–165, 1980.

[52] Wilensky R. L, Tranum-Jensen J, Coronel R, Wilde A. A, Fiolet J. W, and Janse M. J. The subendocardial border zone during acute ischemia of the rabbit heart: an electrophysiologic, metabolic, and morphologic correlative study. *Circ*, 74(5): 1137–1146, 1986. doi: 10.1161/01.CIR.74.5.1137. http://circ.ahajournals.org/content/74/5/1137.

[53] Wolferth C. C, Bellet S, Livezey M. M, and Murphy F. D. Negative displacement of the rs-t segment in the electrocardiogram and its relationships to positive displacement; an experimental study. *Am Heart J*, 29(2):220–245, 1945. ISSN 0002-8703. doi: https://doi.org/10.1016/0002-8703(45)90519-9. http://www.sciencedirect.com/science/article/pii/0002870345905199.

[54] Holland R. P and Brooks H. Precordial and epicardial surface potentials during Myocardial ischemia in the pig. A theoretical and experimental analysis of the TQ and ST segments. *Circ Res*, 37(4):471–480, 1975. doi: 10.1161/01.RES.37.4.471. http://circres.ahajournals.org/content/37/4/471.

[55] Rodríguez B, Trayanova N, and Noble D. Modeling cardiac ischemia. *Ann NY Acad Sci*, 1080(1):395–414, 2006. doi: 10.1196/annals.1380.029. http://dx.doi.org/10.1196/annals.1380.029.

[56] Ferrero J. M, Trenor B, Rodríguez B, and Saiz J. Electrical acticvity and reentry during acute regional myocardial ischemia: Insights from simulations. *Int J Bifurcat Chaos*, 13(12):3703–3715, 2003. doi: 10.1142/S0218127403008806. http://doi.org/10.1142/S0218127403008806.

[57] Tice B. M, Rodriguez B, and Trayanova N. A. Arrthythmogenicity of transmural heterogeneities in a realistic model of regional ischemia. *Heart Rhythm*, 2:1547–5271, 2005. doi: 10.1016/j.hrthm.2005.02.820. http://dx.doi.org/10.1016/j.hrthm.2005.02.820.

[58] Weiss D. L, Ifland M, Sachse F. B, Seemann G, and Dössel O. Modeling of cardiac ischemia in human myocytes and tissue including spatiotemporal electrophysiological variations. *Biomed Eng*, 54, 2009. doi: 10.1515/BMT.2009.016. http://doi.org/10.1515/BMT.2009.016.

[59] Heidenreich E. A, Ferrero J. M, and Rodríguez J. F. *Modeling the Human Heart Under Acute Ischemia*, pages 81–103. Springer Netherlands, Dordrecht, 2012. ISBN 978-94-007-4552-0. doi: 10.1007/978-94-007-4552-0_4. https://doi.org/10.1007/978-94-007-4552-0_4.

[60] Mena A, Migliavacca F, M F. J, and Rodriguez Matas J. F. Vulnerability in regionally ischemic human heart. Effect of the extracellular potassium concentration. *J Comput Sci*, 24:160–168, 2018. doi: 10.1016/j.jocs.2017.11.009. https://doi.org/10.1016/j.jocs.2017.11.009.

[61] Dutta S, Mincholé A, Zacur E, Quinn T. A, Taggart P, and Rodriguez B. Early afterdepolarizations promote transmural reentry in ischemic human ventricles with reduced repolarization reserve. *Prog Biophys Mol Bio*, 120(1):236–248, 2016. doi: https://doi.org/10.1016/j.pbiomolbio.2016.01.008. http://www.sciencedirect.com/science/article/pii/S0079610716000109.

[62] Coronel R, Fiolet J. W, Wilms-Schopman F. J, Schaapherder A. F, Johnson T. A, Gettes L. S, and Janse M. J. Distribution of extracellular potassium and its relation to electrophysiologic changes during acute myocardial ischemia in the isolated perfused porcine heart. *Circ*, 77(5):1125–1138, 1988. doi: 10.1161/01.CIR.77.5.1125. http://circ.ahajournals.org/content/77/5/1125.

[63] A. N. ATP-regulated K^+ channels in cardiac muscle. *Nature*, 305(5930):147–148, 1983. doi: 10.1038/305147a0. http://doi.org/10.1038/305147a0.

[64] Yatani A, Brown A. M, and Akaike N. Effect of extracellular ph on sodium current in isolated, single rat ventricular cells. *J Membrane Biol*, 78(2):163–168, Jun 1984. doi: 10.1007/BF01869203. https://doi.org/10.1007/BF01869203.

[65] Garny a, Kohl P, and Noble D. Cellular Open Resource (COR): a public Cellml based environment for modeling biological function. *Int J Bifurcat Chaos*, 13(12):3579–3590, 2003. doi: 10.1142/S021812740300882X. http://www.worldscientific.com/doi/abs/10.1142/S021812740300882X.

[66] Miller A. K, Marsh J, Reeve A, Garny A, Britten R, Halstead M, Cooper J, Nickerson D. P, and Nielsen P. F. An overview of the CellML API and its implementation. *BMC Bioinformatics*, 11(1):178, April 2010. ISSN 1471-2105. doi: 10.1186/1471-2105-11-178. https://doi.org/10.1186/1471-2105-11-178.